

adsorption of slightly less material per cycle (by ~ 2 Å). The refractive index assumed, 1.5, was representative of the values measured ellipsometrically (1.48 to 1.59) on structures greater than 50 nm in thickness. The measured refractive index increased with increasing multilayer thickness.

19. The concentration of the polymer solution was diluted in increments from 20 to 0.05% (w/w), and in response, the amount of polymer adsorbed per cycle decreased monotonically from 2.1 to 0.1 nm. The amount of hectorite adsorbed per cycle correspondingly fell monotonically from 2.7 to 0.6 nm.
20. Adsorption of $(\text{CH}_3\text{O})_3\text{Si}(\text{CH}_2)_3\text{N}(\text{CH}_3)_3\text{Cl}$ onto a silicon wafer from a chloroform solution gave a covalently bound layer with an ellipsometric thickness of ~ 6 Å.
21. G. Decher *et al.*, *Polym. Prepr.* **34**, 745 (March 1993); Y. Lvov, H. Haas, G. Decher, H. Möhwald, A. Kalachev, *J. Phys. Chem.* **97**, 12835 (1993); R. K. Iler, *J. Colloid Interface Sci.* **21**, 569 (1966).
22. H. Byrd *et al.*, *J. Am. Chem. Soc.* **116**, 295 (1994).
23. Data were obtained on a Philips APD 3720 powder x-ray diffractometer with $\text{Cu K}\alpha$ radiation.
24. The average growth in thickness per cycle as determined by ellipsometry was not an even multiple of the 1.4-nm periodicity revealed by XRD. This result reflects the fact that ellipsometry gives the average thickness within an illuminated spot (~ 1 mm² in area). A measured increase in thickness of 3.6 nm may indicate that in any one cycle, some regions within the illuminated spot gained two layers, while others gained three.
25. H. S. Peiser *et al.*; Eds., *X-Ray Diffraction by Polycrystalline Materials* (Wright, Bristol, UK, 1955), p. 466.
26. V. A. Drits and C. Tchoubar, *X-Ray Diffraction by Disordered Lamellar Structures* (Springer-Verlag, New York, 1990), pp. 21–22.
27. B. E. Warren, *X-Ray Diffraction* (Addison-Wesley, Reading, MA, 1969), pp. 251–254.
28. The XRD data presented in the original manuscript of this report had two additional features: a very sharp peak at 33.0° ($d = 0.27$ nm), and a broad, very low intensity peak at $\sim 13.3^\circ$ ($d = 0.66$ nm). Both of these features were absent if samples were rinsed more extensively both during multilayer formation and shortly before XRD analysis. The full width at half height of the (001) peak in that pattern was 2.0° , indicating a domain size of 3.6 nm.
29. W. M. R. Divigalpiya, R. F. Frindt, S. R. Morrison, *Science* **246**, 369 (1989).
30. The AFM image was acquired with a Parks Scientific Instruments Autoprobe cp with an Ultra-lever (silicon) probe tip.
31. We have recently formed PDDA-hectorite multilayers on gold and on copper and have formed multilayered structures on silicon using a different polyelectrolyte, poly(*N*-methyl-4-vinylpyridinium bromide).
32. M. D. Porter, T. B. Bright, D. L. Allara, C. E. D. Chidsey, *J. Am. Chem. Soc.* **109**, 3559 (1987).
33. H. Lee, L. J. Kepley, H.-G. Hong, S. Akhter, T. E. Mallouk, *J. Phys. Chem.* **92**, 2597 (1988).
34. S. Steinberg *et al.*, *Science* **260**, 656 (1993).
35. H.-Y. Liu, F.-R. F. Fan, A. J. Bard, *J. Electrochem. Soc.* **132**, 2666 (1985); M. H. B. Stiddard, *Thin Solid Films* **94**, 1 (1982); R. Waser and K. G. Weil, *J. Electroanal. Chem.* **150**, 89 (1983); A. Putnam, B. L. Blackford, M. H. Jericho, M. O. Watanabe, *Surf. Sci.* **217**, 276 (1989).
36. D. Li *et al.*, *J. Am. Chem. Soc.* **112**, 7389 (1990).
37. P. Day and R. D. Ledsham, *Mol. Cryst. Liq. Cryst.* **86**, 163 (1982).
38. C.-G. Wu, M. G. Kanatzidis, H. O. Marcy, D. C. DeGroot, C. R. Kannewurf, in *Lower-Dimensional Systems and Molecular Electronics*, R. M. Metzger, P. Day, G. C. Papavassiliou, Eds. (Plenum, New York, 1991), pp. 427–433.
39. J. F. Bringley and B. A. Averill, *Chem. Mater.* **2**, 180 (1990).
40. We gratefully acknowledge O. Shaffer for assistance in obtaining AFM images, D. Simpson for helpful discussions regarding the interpretation of x-ray diffractograms (obtained with the assistance

of G. Yasko), A. Miller and D. Carey for technical assistance with the x-ray photoemission spectroscopic analysis, and Lehigh University for supporting the Scienta ESCA-300 Laboratory. Silicon wafers used as substrates were donated by WaferNet. The synthetic hectorite was donated by

Laporte Industries to D. Hseih, who kindly provided us with a sample. E.R.K. gratefully acknowledges financial support from AT&T Laboratories in the form of a Ph.D. Scholarship.

16 February 1994; accepted 16 May 1994

Size Dependence of a First Order Solid-Solid Phase Transition: The Wurtzite to Rock Salt Transformation in CdSe Nanocrystals

S. H. Tolbert and A. P. Alivisatos

Measurements of the size dependence of a solid-solid phase transition are presented. High-pressure x-ray diffraction and optical absorption are used to study the wurtzite to rock salt structural transformation in CdSe nanocrystals. These experiments show that both the thermodynamics and kinetics of this transformation are altered in finite size, as compared to bulk CdSe. An explanation of these results in the context of transformations in bulk systems is presented. Insight into the kinetics of transformations in both bulk and nanocrystal systems can be gained.

Studies of phase transitions in condensed phases have generally assumed that pressure, temperature, and composition are the only variables of importance in determining stable states of materials. The reduction of melting temperature in finite size clusters (1, 2), however, has proven that the physical extent of a material can also be an important variable in determining transition points. Recently, studies of clusters in both the gas and condensed phases have led to numerous instances in which one bonding geometry appears to be favored over others in finite size, as compared to the bulk (3). To help understand these observations, we investigated the relative stability of two different solid bonding geometries in clusters as a function of the size. Our goal was to force a nanocrystal system between two solid structures and measure the energy difference between them. We achieved this goal through the application of very high pressures.

This study of the size dependence of a solid-solid phase transition also reveals important dynamical effects that are not observed in size-dependent melting. In a bulk system, the thermodynamic definition of a phase transition is the point where the fluctuation length scale diverges. In a nanocrystal, this length scale is intrinsically limited by the size of the crystallite. Additionally, in most inorganic solid-solid transitions, there is a substantial barrier to transition at room temperature. As a consequence, the bulk solid converts at a pressure well above its thermodynamic transition pressure. This barrier is usually related to the fragmentation of bulk materials into

finite domains upon transition. Because nanocrystals are substantially smaller than these domains, it is likely that the barriers to transition will be altered at finite sizes. By studying structural transformations in nanocrystals, we can learn about the nature of the barrier and the dynamics of the transition in bulk as well as in nanocrystals.

While understanding the altered stability in finite size is of fundamental interest, it also has practical implications in a variety of fields ranging from microelectronics and materials science to geophysics. Variation in stability with size could provide the materials scientist with a method for control of the properties of materials. By using nanocrystals whose surface can be deliberately altered, one may be able to vary the phase diagram at will. In geophysics as well, the notion of a domain size dependence of high-pressure and high-temperature phase transitions could affect our understanding of stable states.

The system that we have chosen for these experiments is CdSe semiconductor nanocrystals. Recent developments in synthetic methods make this a particularly well controlled and characterized test system. Nearly monodisperse, spherical nanocrystals ranging in radius from 10 to 30 Å can now be produced (4, 5). Unlike the many nanocrystalline materials that appear to be amorphous, these nanocrystals have a wurtzite structure and are highly crystalline, with less than one fault per crystallite (6). The fact that these nanocrystals are synthesized in the condensed phase adds an important degree of control to the sample preparation by allowing for chemical surface derivatization. This combination of properties makes this an ideal system for testing the effect of finite size on stable structures.

Bulk CdSe undergoes a phase transition

Materials Science Division, Lawrence Berkeley Laboratory, and Department of Chemistry, University of California, Berkeley, CA 94720, USA.

from a wurtzite to a rock salt structure at 2 GPa (7). However, previous studies show that CdS (8, 9) and CdSe (10–12) nanocrystals are stable to pressures two to three times higher than the bulk. Similar results have been obtained for GaAs–AlAs superlattices (13). We combined high-pressure x-ray diffraction and optical absorption to thoroughly assess both the high-pressure phase structure and crystallinity and to measure the size dependence of the phase transition pressure. This combination of experiments provides a unique perspective on the thermodynamics and kinetics of this solid-solid phase transformation.

The CdSe nanocrystals were synthesized by a modification of the method of Murray and Bawendi (4, 5) and were characterized by x-ray diffraction, transmission electron microscopy, optical absorption, Raman spectroscopy, and small angle x-ray scattering. Nanocrystal samples were dissolved in 4-ethyl-pyridine, a solvent that is a reasonable hydrostatic pressure medium to pressures in excess of 10 GPa and in which the nanocrystals are highly soluble. Pressure was determined by standard ruby fluorescence tech-

niques (14). High-pressure optical absorption studies were performed with a Mao-Bell-style (15) diamond anvil cell (DAC) in combination with a Cary model 118 ultraviolet (UV)-visible spectrometer. High-pressure x-ray diffraction experiments were carried out on wiggler beam line 10-2 at the Stanford Synchrotron Radiation Laboratory with a Merrill-Bassett-style diamond cell with Be rockers. Focused monochromatic 12.5-keV x-rays were collimated and apertured to 0.1 mm through a series of three slits and pin holes. The x-ray energy was below the Se absorption edge (12.6 keV), thus minimizing Se absorption and $K\alpha$ fluorescence. Debye-Scherrer rings were angle-integrated to produce the data presented here.

High-pressure diffraction data on bulk CdSe (Fig. 1A) show a phase transition from a four-coordinate wurtzite to a six-coordinate rock salt structure, which is complete by 3.5 GPa. The recovered phase is a mixture of the two four-coordinate structures, zinc blende and wurtzite. This is in good agreement with previous reports on bulk CdSe (7, 16). After multiple transitions, the diffraction peaks broaden, indicating a reduction of the average

domain size from instrument-limited in the original sample (greater than 600 Å), to about 300 Å in the rock salt phase, down to only 100 Å in the recovered zinc blende–wurtzite mix.

Diffraction data were obtained on nanocrystals 22 Å in radius consisting of about 2000 atoms each (Fig. 2). In comparison with the bulk data (Fig. 1A), the peaks are significantly broadened by the finite size of the crystallites (Debye-Scherrer broadening). The sample retained the wurtzite structure to well above the bulk stability limit of 3 GPa (Fig. 2A). Above 6 GPa, however, the sample did start to transform; by 7.5 GPa, a clean rock salt pattern was observed. The system showed significant hysteresis upon release of pressure (Fig. 2B), with the rock salt structure persisting down to below 1 GPa. By the return to atmospheric pressure, a wurtzite–zinc blende pattern was recovered. It is not experimentally possible to determine if this pattern results from a mixture of pure zinc blende and pure wurtzite particles or from nanocrystals that are actually of a mixed structure (17). In sharp contrast to the bulk CdSe data (Fig. 1A), there was no significant decrease in crystalline domain size in the nanocrystals upon multiple transitions (Fig. 1B). This important result leads to the conclusion that nanocrystals are coherently transforming from one solid structure to another.

Changes in the optical absorption spectra with pressure correlate well with the structural phase transition observed by x-ray diffraction. High-pressure UV-visible spectroscopy can thus be used to determine the phase transition

Fig. 1. (A) High-pressure x-ray diffraction patterns obtained on bulk CdSe. Average domain size and pressure are indicated on the figure. Recovered spectra are at atmospheric pressure. The data show a decrease in x-ray domain size (increase in peak width) with subsequent transitions. Intensity anomalies in the original wurtzite pattern are attributed to single crystal diffraction events caused by the limited size of the sample. (B) Analogous data for 4.4-nm-diameter CdSe nanocrystals. Almost no change in x-ray domain size was observed upon multiple transitions. ZB-WZ refers to a mixture of the closely related zinc blende and wurtzite structures. Arrows indicate diffraction from the high-pressure-cell metal gasket. The x-ray wavelength was 0.9939 Å.

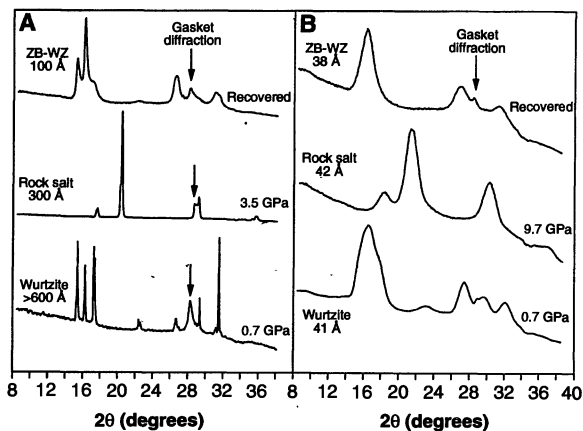


Fig. 2. (A) Changes in x-ray diffraction pattern with increasing pressure for 4.4-nm-diameter CdSe nanocrystals. The data show an upstroke transition pressure near 6.3 GPa that is about twice the bulk CdSe upstroke transition pressure of 3 GPa. (B) Changes in x-ray diffraction pattern with decreasing pressure for the same 4.4-nm nanocrystals. Large hysteresis is observed. ZB-WZ refers to a mixture of the closely related zinc blende and wurtzite structures; atm is atmospheric pressure. Diffraction peaks are indexed on the figure. Labeled arrows indicate diffraction from the high-pressure-cell metal gasket. The x-ray wavelength was 0.9939 Å.

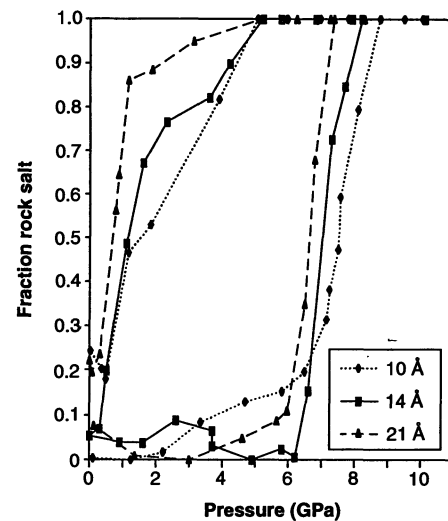
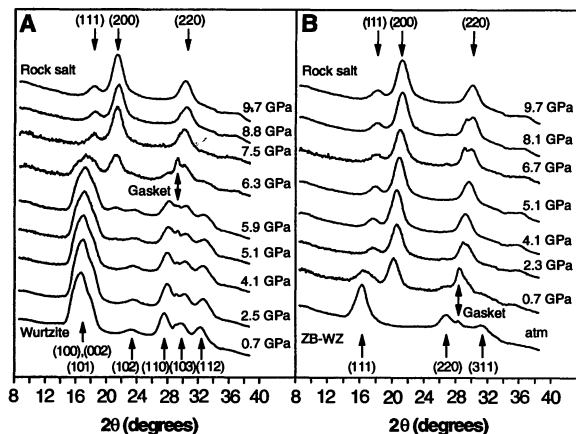


Fig. 3. Hysteresis curves for three sizes of CdSe nanocrystals, corrected for changes in optical density caused by deformation of the DAC gasket with pressure. Data were obtained by integration of the low-pressure-phase optical absorption features. "Fraction rock salt" is defined as 1 - (fractional wurtzite-phase absorption). Phase transition pressures are assigned to the midpoints of these hysteresis curves.

pressure for a variety of nanocrystal sizes. The wurtzite phase has a direct gap and thus has allowed electronic transitions at visible wavelengths. Confinement of the excitonic state by the intrinsic size of the nanocrystal produces a spectrum with multiple discrete features. In contrast, the rock salt phase has an indirect gap and thus shows no sharp features. By integration of the direct gap features, it is possible to assess the degree of transformation or recovery of a sample as a function of pressure and quantify the hysteresis. Consistent with this being a Martensitic transformation, we have observed no change in this hysteresis on time scales ranging from minutes to weeks. The data (Fig. 3) show a clear shift to higher upstroke transition pressure with decreasing crystallite size. Although the widths of the hysteresis curve do not change significantly with size, some change with size is seen in the slope of the recovery curve. Because the hysteresis widths are significantly broader than those observed in bulk CdSe, the curves suggest a qualitative difference in the kinetics of the transformation in finite size.

If the phase transition pressure is assigned to the midpoint of the hysteresis curve, the size dependence of the phase transition pressure can be determined (Fig. 4). By analogy with melting in nanocrystals, a numerical description of the changes in transition pressure can be obtained in terms of differences in surface energies of the two phases (6, 10) (solid line, Fig. 4). The essential physics, however, can be more easily understood graphically by considering the energy-volume plane (8, 18) (Fig. 5). On this plane, each phase of CdSe can be represented by an energy-volume curve, which can be experimentally determined by integrating the pressure-volume curves ($E = -\int PdV$). The ver-

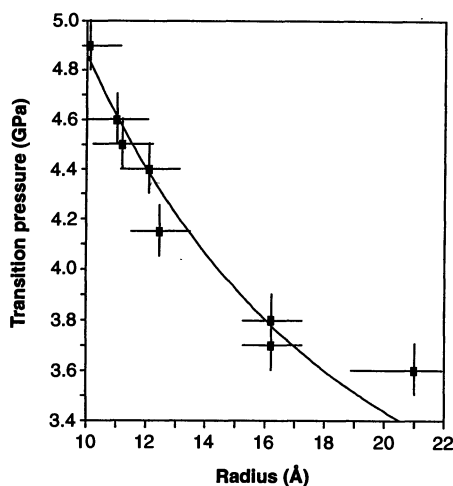


Fig. 4. Wurtzite-to-rock salt transformation pressure as a function of nanocrystal radius. The transition pressures are defined according to Fig. 3. The solid line is a fit to a thermodynamic model explained in the text.

tical offset of the bulk rock salt curve with respect to the bulk wurtzite curve is determined by the condition that both curves must be tangent to a line that corresponds to the phase transition pressure ($-dU/dV = P$). In the case of nanocrystals, however, the wurtzite-phase curves are elevated with respect to the bulk wurtzite curve by a surface energy term γ . Experimentally (6), this term varies with radius r as $\gamma = c_1 + c_2/(r^2)$, where c_1 can be related to a bulk surface tension and c_2 is a term proportional to the curvature of the nanocrystal surface. The nanocrystal wurtzite curves in Fig. 5 are thus offset from the bulk wurtzite curves by the increases in surface area and surface energy that accompany decreasing size. An elevation in the structural phase transition pressure with decreasing nanocrystal size can be explained by the hypothesis that the surface energy in the rock salt phase, for any given crystallite size, is actually higher than that for the wurtzite phase. The slope of the line needed to connect the rock salt and wurtzite curves thus increases with decreasing nanocrystal size.

Because the experimentally determined phase transition pressure is the slope of the line connecting the wurtzite and rock salt phase nanocrystal curves, only the surface energy for the rock salt phase needs to be optimized to numerically fit the data to this model. The line shown in Fig. 4 was obtained with an experimentally determined wurtzite-phase surface energy (19) of $\gamma_{WZ} = 0.34 + 84/r^2$ and an optimized rock salt-phase surface energy of $\gamma_{RS} = 0.63 + 83/r^2$ (in newtons per meter with r in angstroms). However, the basic observation that the rock salt surface energy is higher than the wurtzite energy is in contradiction to previous calculations (20), which predict $\gamma_{WZ} > \gamma_{RS}$. A possible explanation for this contradiction can be gained by considering the kinetics of the phase transformation.

In a perfect thermodynamic model, phase transitions occur at exactly one temperature and pressure and are completely reversible. For solids in general, however, this is not observed. High-pressure phase transitions are generally hysteretic and occur over a range of pressures. In bulk systems, this hysteresis is explained in terms of nucleation dynamics (21). A nucleus of the rock salt phase in the wurtzite-phase lattice is assumed to be destabilized by a rock salt-wurtzite interface energy, and thus, extra energy (PdV) must be put into the stabilization of a rock salt nucleus before a transition can occur. On the reverse transition, the wurtzite-phase nucleus is destabilized by the same rock salt-wurtzite interface energy, and so the pressure must be lowered an equivalent amount beyond the equilibrium transition pressure to induce the reverse transition. The broadening of the diffraction peaks with successive transformations for bulk

CdSe (Fig. 1A) is indicative of this type of mechanism, where multiple nucleation sites cause a decrease in crystalline domain size upon transition. The absence of a significant decrease in domain size for the nanocrystals after multiple transitions (Fig. 1B) argues that the total size of the nanocrystals is smaller than the smallest stable nuclei in the bulk. These results place a lower limit on the size of critical nuclei in bulk CdSe and are thus of fundamental interest to understanding nucleation dynamics in bulk solid-solid phase transitions (22).

The existence of broad hysteresis curves (Fig. 3), however, indicate that despite the lack of a traditional nucleation barrier to transition, some significant barrier is still present. The rearrangement of surface atoms and surface-bound ligands to accommodate the new interior structure is one candidate. The observation that the shapes of the hysteresis curves are dependent on size (Fig. 3) supports this idea.

Other important dynamic effects in these structural transformations can be understood by considering the motions of individual atoms along the transition path. The exterior shape of a crystal is dictated by the bonding geometry of the unit cell. In a pressure-induced structural transformation at room temperature, the interior bonding geometry of the crystal changes. The thermal energy, however, is small compared to the barrier to surface diffusion. As a result, in both the bulk solid and the nanocrystals,

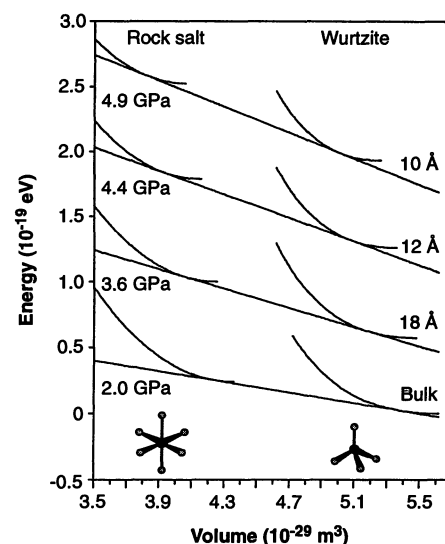


Fig. 5. Energy-volume curves for bulk CdSe and three sizes of CdSe nanocrystals in both the wurtzite and the rock salt phases. Nanocrystal curves are offset with respect to the bulk because of the surface energy in the nanocrystals. The offset of the rock salt curves with respect to the wurtzite curves determines the phase transition pressure. Transition pressures and nanocrystal sizes are indicated on the figure.

the solid cannot attain its true equilibrium shape after transformation to the high-pressure phase. The bulk solid fragments into domains and the nanocrystal converts coherently from one shape to another. In the present case, nearly spherical nanocrystals with low-index surfaces convert to prolate ellipsoids with many high-index surfaces. This effect arises because the connectivity of the atoms cannot be altered. Burdett has shown that transition paths of this type can be viewed as three-dimensional Peierls distortions (23). This effect then explains the seemingly anomalous results that the rock salt-phase surface energy required to fit the nanocrystal size dependence of the phase transition was much larger than that expected for low-index rock salt-phase CdSe.

In the case of nanocrystals, where the surface energy makes a major contribution to the total free energy of the system, the transition path can actually determine the final state of the system. In a true equilibrium experiment, where path effects are not important, the rock salt surface energy would probably be less than that of the wurtzite, and a depression of the phase transition pressure would actually be observed. Thus, path effects play a major role in both the dynamics and the ultimate stable phases of nanometer-scale materials. Because of this, nanocrystals provide an opportunity to observe the effects of the transition path, which are masked in bulk systems. The potential is great for use of these and related experiments on nanocrystals to gain new understanding of the dynamics of solid-solid phase transformations in bulk systems.

Although these basic conclusions are general to wurtzite-phase nanocrystals, the specific surface energies reported here are probably influenced by the choice of surface ligand, 4-ethyl-pyridine. While the possibility does exist to actually change the ordering of wurtzite and rock salt surface energies through the use of an appropriate ligand, no significant changes in surface energy ordering are observed within the range of ligands we are currently able to use (Lewis bases). The question of surface modification aside, the present work demonstrates that a solid-solid phase transition smoothly evolves into a coherent molecular isomerization in finite size.

REFERENCES AND NOTES

1. A. N. Goldstein, C. M. Echer, A. P. Alivisatos, *Science* **256**, 1425 (1992).
2. C. J. Coombes, *J. Phys.* **2**, 441 (1972); P. Buffat and J.-P. Borel, *Phys. Rev. A* **13**, 2287 (1976).
3. The most obvious and striking example of this type of behavior is the fullerene cluster C_{60} [H. W. Kroto, J. R. Heath, S. C. O'Brein, R. F. Curl, R. E. Smalley, *Nature* **318**, 162 (1985)]. Metallic and ionic clusters are also expected to show this type

- of behavior [B. K. Teo, X. Shi, H. Zhang, *J. Am. Chem. Soc.* **113**, 4329 (1991); J. Deifenbach and T. P. Martin, *J. Chem. Phys.* **83**, 4585 (1985)].
4. C. B. Murray, D. J. Norris, M. G. Bawendi, *J. Am. Chem. Soc.* **115**, 8706 (1993).
5. J. E. Bowen Katari, V. L. Colvin, A. P. Alivisatos, *J. Phys. Chem.* **98**, 4109 (1994).
6. S. H. Tolbert and A. P. Alivisatos, in preparation.
7. For these experiments, we defined the thermodynamic phase transition pressure as the midpoint of the hysteresis curve, or equivalently, the average of the upstroke and downstroke transition pressures. This produces a bulk CdSe transition pressure of 2 GPa, in comparison with the upstroke value of 3 GPa. Experiments on bulk CdSe that show full hysteresis data include A. L. Edwards and H. G. Drickamer, *Phys. Rev.* **122**, 3196 (1962); A. Onodera, *Rev. Phys. Chem. Jpn* **39**, 65 (1969); and W. C. Yu and P. J. Gielisse, *Mater. Res. Bull.* **6**, 621 (1971).
8. M. Haase and A. P. Alivisatos, *J. Phys. Chem.* **96**, 6756 (1992).
9. X. S. Zhao, J. Schroeder, P. D. Persans, T. G. Bilodeau, *Phys. Rev. B* **43**, 12580 (1991).
10. S. H. Tolbert and A. P. Alivisatos, in *Nanophase Materials: Synthesis-Properties-Applications*, G. C. Hadjipanayis and R. W. Siegel, Eds. (NATO Advanced Study Institutes Series, Kluwer Academic, Dordrecht, Netherlands, 1993), pp. 471-482.
11. ———, *Z. Phys. D* **26**, 56 (1993).
12. A. P. Alivisatos, T. D. Harris, L. E. Brus, A. Jayaraman, *J. Chem. Phys.* **89**, 5979 (1988).
13. L. J. Cui, U. D. Venkateswaran, B. A. Weinstein, F. A. Chambers, *Phys. Rev. B* **45**, 9248 (1992).
14. J. D. Barnett, S. Block, G. J. Piermarini, *Rev. Sci. Instrum.* **44**, 1 (1973).
15. H. K. Mao and P. M. Bell, *Carnegie Inst. Washington Yearb.* **75**, 824 (1976).
16. A. N. Mariano and E. P. Warekoi, *Science* **142**, 672 (1963).

17. Although either a mixture of pure zinc blende and pure wurtzite nanocrystals or nanocrystals of a mixed phase could produce the observed pattern, the observation of coherent transformations in this system argues in favor of the first option.
18. For a review of these ideas, see R. S. Berry, S. A. Rice, J. Ross, *Physical Chemistry* (Wiley, New York, 1980), pp. 875-883.
19. This value was obtained by fitting lattice contraction data versus nanocrystal size with the use of a simple Laplace law formalism (6).
20. B. N. Oshcherin, *Phys. Status Solidi A* **34**, K181 (1976).
21. R. E. Hanneman, M. D. Banus, H. C. Gatos, *J. Phys. Chem. Solids* **25**, 293 (1964).
22. U. D. Venkateswaran, L. J. Cui, B. A. Weinstein, F. A. Chambers, *Phys. Rev. B* **45**, 9237 (1992).
23. J. K. Burdett and T. J. McLarnan, *J. Chem. Phys.* **75**, 5765 (1981); J. K. Burdett, *Prog. Solid State Chem.* **15**, 173 (1984).
24. We thank M. Nicol, S. Mustonen, and A. Kadavanih for their technical assistance with this experiment. A.P.A. acknowledges an Alfred P. Sloan Foundation fellowship. This work has been partially supported by the donors of the Petroleum Research Fund, administered by the American Chemical Society, and by the Director, Office of Energy Research, Office of Basic Energy Sciences, Materials Science Division, of the U.S. Department of Energy (DOE) under contract DE-AC03-76SF0098. The experiments were performed using the facilities of the University of California-Lawrence Livermore National Lab Participating Research Team at the Stanford Synchrotron Radiation Laboratory, which is operated by the DOE, Division of Chemical Sciences.

24 February 1994; accepted 17 May 1994

First Principles Determination of the Effects of Phosphorus and Boron on Iron Grain Boundary Cohesion

Ruqian Wu, A. J. Freeman, G. B. Olson

Toward an electronic level understanding of intergranular embrittlement and its control in steels, the effects of phosphorus and boron impurities on the energy and electronic properties of both an iron grain boundary and its corresponding intergranular fracture surface are investigated by the local density full potential augmented plane wave method. When structural relaxations are taken into account, the calculated energy difference of phosphorus in the two environments is consistent with its measured embrittlement potency. In contrast to the nonhybridized interaction of iron and phosphorus, iron-boron hybridization permits covalent bonding normal to the boundary contributing to cohesion enhancement. Insights into bonding behavior offer the potential for new directions in alloy composition for improvement of grain boundary-sensitive properties.

The mechanical properties of ultrahigh-strength steels are often limited by the cohesion of crystal grain boundaries as influenced by the intergranular segregation of various metalloid impurities such as P and S. A thermodynamic theory developed by

Rice and Wang (1, 2) describes the mechanism of metalloid-induced intergranular embrittlement through the competition between plastic crack blunting and brittle boundary separation. While crystal plasticity considerations show interesting directional effects on the relative ease of crack tip blunting verified in critical bicrystal experiments, the most striking result of the analysis is the prediction that the potency of a segregating solute in reducing the "Griffith work" of brittle boundary separa-

R. Wu and A. J. Freeman, Department of Physics and Astronomy, Northwestern University, Evanston, IL 60208, USA.

G. B. Olson, Department of Materials Science and Engineering, Northwestern University, Evanston, IL 60208, USA.